Int. J. Heat Mass Transfer. Vol. 21, pp. 1369–1377

0017-9310/78/1101-1369 $02.00/0

HEAT TRANSFER AND PRESSURE DROP FOR A STAGGERED WALL-ATTACHED ARRAY OF CYLINDERS WITH TIP CLEARANCE

E. M. SPARROW and J. W. RAMSEY
Department of Mechanical Engineering, University of Minnesota,
Minneapolis, MN 55455, U.S.A.

(*Received* 6 *February* 1978 *and in revised form* 15 *March* 1978)

Abstract—Experiments have been performed to determine the detailed row-by-row heat-transfer characteristics of a staggered array of circular cylinders situated in a crossflow of air in a flat rectangular duct. The cylinders were attached perpendicular to one of the principle walls of the duct, with a clearance space between the free ends of the cylinders and the other principle wall. The heat-transfer coefficients were obtained by applying the analogy between heat and mass transfer to mass-transfer coefficients measured via the napthalene sublimation technique. Pressure measurements were also made to determine the incremental pressure drop due to the presence of the cylinder array. The row-by-row transfer coefficients were found to vary only in the initial rows and to attain a constant fully developed value for the fourth and all subsequent rows. The fully developed transfer coefficients are quite insensitive to cylinder height (i.e. to the extent of the tip clearance), increasing moderately as the height increases (and the clearance decreases). On the other hand, the array pressure drop increases markedly with increasing cylinder height.

NOMENCLATURE

A, mass-transfer area;
A_{min}, minimum flow cross sectional area;
D, cylinder diameter;
D_h, hydraulic diameter of unobstructed duct;
$\mathscr{D}$, naphthalene–air diffusion coefficient;
H, duct height;
h, cylinder height;
K, mass-transfer coefficient, $(\dot{M}/A)/\rho_{nw}$;
K_p, pressure coefficient per row, equation (6);
$\dot{M}$, mass-transfer rate;
N, number of rows;
Nu, Nusselt number;
Nu^*, Nusselt number for tube bank;
$(dp/dx)_{duct}$, pressure gradient in unobstructed duct;
$(dp/dx)_{TS}$, pressure gradient in test section;
Δp_{array}, incremental pressure drop due to cylinder array;
Re, Reynolds number, $V_{max}D/\nu$;
Re_{duct}, Reynolds number of unobstructed duct, $\bar{V}D_h/\nu$;
Sc, Schmidt number, $\nu/\mathscr{D}$;
Sh, Sherwood number, $KD/\mathscr{D}$;
Sh^*, Sherwood number for tube bank;
V_{max}, superficial maximum velocity, equation (3);
$\bar{V}$, mean velocity in unobstructed duct;
$\dot{w}$, mass flow rate of air;
x, streamwise coordinate.

Greek symbols

ν, kinematic viscosity;
ρ, density;
ρ_{nw}, naphthalene vapor concentration at cylinder surface.

INTRODUCTION

ONE OF the techniques for enhancing the heat transfer from a wall to a fluid is to increase the transfer area by means of an array of wall-attached cylinders (e.g. rods, wires) mounted perpendicular to the wall. Extended surfaces of this type are often referred to as pin fins. In typical heat exchanger applications, the fluid passes in crossflow through the array of cylinders. As will be discussed shortly, there is very little information in the literature about the heat transfer and pressure drop characteristics of such arrays.

In the present research, experiments have been performed to determine the detailed row-by-row heat-transfer characteristics of an array of wall-attached cylinders situated in a crossflow of air. Detailed pressure measurements were also made from which the pressure drop characteristics were determined. The experiments were performed with the cylinder array position in a flat rectangular duct, with the respective cylinders seated in receptacles in the duct floor. Three arrays, each characterized by a different cylinder height, were employed. Correspondingly, each array had a different degree of clearance between the tops of the cylinders and the upper wall of the duct. For all arrays, the cylinders were arranged in a staggered pattern on equilateral triangular centers.

The experimental set-up can be seen from the photograph presented in Fig. 1. The photo was taken with the top wall of the test section removed so as to reveal the array of cylinders.

The pattern of fluid flow through and above the array is expected to be highly complex, with the open

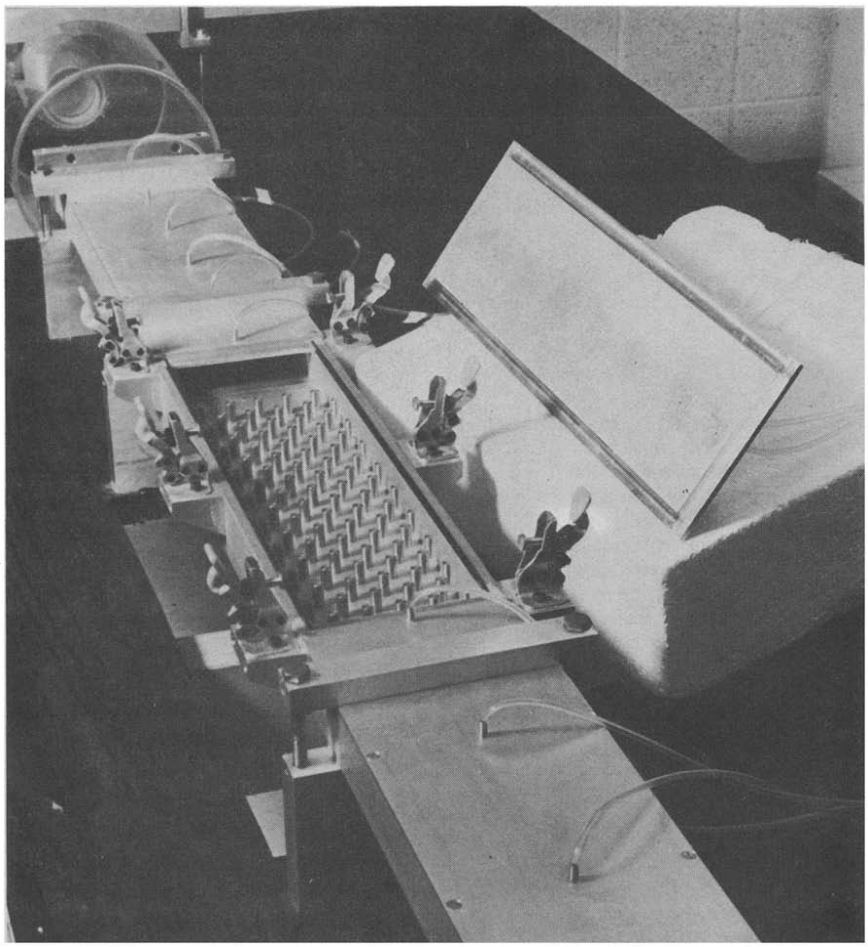

FIG. 1. Photograph of the test section with the upper wall removed.

clearance space above the cylinders playing an important role. The flow cross section is made up of the inter-cylinder spaces and the open clearance spaces. In seeking the path of least resistance, the fluid will favor the open clearance in preference to the relatively confined inter-cylinder spaces. As a result, the mean velocity of the flow passing through the inter-cylinder spaces will be smaller than that of the flow in the open clearance space.

The flow field adjacent to the individual cylinders should be strongly affected by the fact that one end is wall-attached while the other end is free. This arrangement should give rise to a transverse flow component (in the direction of the cylinder axis) superposed on the mainflow that passes around the circumference. As a consequence, the wake flow should be strongly three dimensional.

Inasmuch as the array presents a repeating geometry to the flowing fluid and since the flow is confined by the duct walls, it is expected that a hydrodynamically developed regime will be established downstream of a development length. Correspondingly, for the heat transfer, one would expect thermal development to occur in the initial rows of the array followed by a developed regime where the heat-transfer coefficient is a constant from row to row. These expectations will be re-examined during the presentation of results.

To facilitate the research, mass-transfer experiments were performed rather than direct heat-transfer experiments, and the mass-transfer results were converted to heat-transfer results via the well-established analogy between the two processes. The naphthalene sublimation technique was used for the mass-transfer experiments. For the implementation of the technique, individual stainless steel cylinders were coated with a thin film of naphthalene. For any given data run, only a single naphthalene-coated cylinder was positioned in the array—all of the others were uncoated stainless steel. Thus, only that cylinder participated in the mass transfer process. In the various data runs, the participating cylinder was stationed at different positions in the array.

The capability of yielding transfer coefficients for individual cylinders without extraneous end losses is one of the advantages of the naphthalene technique compared with direct heat-transfer experiments. In the latter, conduction losses from the cylinder to the duct wall would have been very difficult to suppress. Another advantage of the naphthalene technique stems from the fact that the mass-transfer boundary condition on

the cylinder surface is analogous to uniform wall temperature in the corresponding heat-transfer problem. A fin with a uniform wall temperature has an efficiency η of unity. Therefore, the heat-transfer coefficients deduced (via analogy) from the mass-transfer experiments correspond to $\eta = 1$. Had direct heat-transfer measurements been performed, the results would have been influenced by the finite fin conductance, and a correction would have been required to convert them to the $\eta = 1$ condition (which is the standard case).

Still another advantage of using the naphthalene technique is the relative simplicity of the experimental apparatus. Furthermore, with reasonable precautions, higher accuracies can be obtained than in heat-transfer experiments.

As already noted, the experiments were performed for three arrays, each with a different cylinder height h. Relative to the cylinder diameter D and to the duct height H, the three cylinder heights were $h/D = 1$, 2, and 3, and $h/H = 0.29$, 0.58, and 0.875. The center-to-center distance between cylinders was equal to $3D$ for all cases, with the centers situated in an equilateral triangular arrangement. The flow was characterized by a Reynolds number based on the cylinder diameter and on a velocity defined via the quotient of the mass flow and the minimum cross sectional area. Overall, the Reynolds number range extended from about 1000 to 9000. The corresponding range of the duct Reynolds number for the flow approaching the array was from 5000 to 35000.

For each array and for each Reynolds number, a succession of experiments was performed to determine the mass-transfer coefficient in each row—starting at the first row and proceeding downstream. In almost all cases, the experiments were not continued beyond the tenth row since the fully developed regime was already well established.

The dimensionless mass-transfer coefficient (i.e. the Sherwood number) for each row was plotted against the row number in order to display the characteristics of the developing and developed regimes. The fully developed Sherwood numbers were converted to Nusselt numbers and reported as a function of the Reynolds number. Comparisons of these results were made with those for crossflow through staggered-array tube bundles having a pitch-diameter ratio equal to that of the present configuration. The measured axial pressure distributions yielded the pressure losses associated with the presence of the cylinder array. These losses were referred to the velocity head and are reported on a per row basis.

A search of the literature failed to reveal experiments comparable to those performed here, neither with regard to methodology nor to the flow configuration. A limited amount of information on pin fins is presented in the Kays–London compendium [1], but the flow configuration and the reported results are of a different sort from those of the present investigation. In the one staggered-array case reported in [1], the pin fins were formed from a continuous length of wire that looped back and forth across the flow cross section. Not only did the wire span the entire cross section between the walls, but it also ran along the walls and, presumably, acted as a trip. In addition to the evident geometrical differences in the flow configurations, it may be noted that [1] presents overall results that encompass both the fins and the base surfaces, whereas those presented here are local and specific to the fins (i.e. the cylinders).

THE EXPERIMENTS

Experimental apparatus

The main component of the apparatus is a flat rectangular duct having cross section dimensions of 8.26×1.91 cm (3.25×0.75 in)—with a resulting aspect ratio of 4.33 to 1 and a hydraulic diameter of 3.1 cm (1.22 in). The initial portion of the duct serves as a hydrodynamic development section and delivers the flow to the test section which houses the cylinder array. Down-stream of the array, in the final portion of the duct, the flow redevelops and re-establishes a fully developed pressure gradient. The respective lengths of the aforementioned sections of the duct are 33, 8, and 14 hydraulic diameters.

The duct exit interfaces with a rectangular-to-circular transition section, which connects to the inlet pipe of a rotameter. The outlet pipe of the rotameter is connected via a control valve to a blower situated in a service corridor outside the laboratory room.

As was already mentioned in connection with Fig. 1, the top wall of the test section is removable. This provision was provided to accommodate the need for frequent access to the test section to install or remove naphthalene-coated cylinders. When in place, the removable section of the wall was held fixed by six quick-release clamps, and a leak-proof seal was accomplished with the aid of O-rings. To gain access to the test section, the clamps were released and the wall removed, all in a matter of seconds. The closing of the test section could be accomplished in a similarly short time. The capability of rapid installation and removal minimizes extraneous sublimation of the naphthalene.

The cylinders of the array are seated in drill holes in the floor of the test section. Provision was made for 18 rows of cylinders, with five cylinders in each row and with staggering of the successive rows. To more closely approximate the infinitely wide array, every other row includes two half cylinders, each flush with one of the side walls, as well as four complete cylinders. The other rows contain five complete cylinders. The spanwise and streamwise distances between the centers of the cylinders are 1.65 and 1.43 cm respectively (0.65 and 0.563 in), which is consistent with an equilateral triangular pattern.

The cylinders are inserted from above and bottom out against a base plate situated immediately below the test section floor. To ensure that the insertion and proper bottoming out of the cylinders is not resisted by air pressure, the underside of the test section floor was relieved to create an air space between the floor and the

bottoming plate. The air space could be vented, when necessary, via a toggle valve.

Stainless steel rod stock, 0.556 cm (7/32 in) in diameter, was used in the fabrication of the cylinders. As noted earlier, experiments were performed with cylinders having heights of one, two, and three diameters exposed to the air stream. The total length of each cylinder was the sum of its exposed height plus the thickness of the test section floor (0.635 cm, 1/4 in). Special care was taken to ensure that the exposed end of each cylinder was finished square. The special fabrication features of the naphthalene-coated cylinders will be discussed shortly.

In each data run, only one naphthalene-coated cylinder was employed. For the majority of the runs, the active cylinder was positioned as close as possible to the spanwise center of the duct to avoid possible end effects due to the side walls. In auxiliary runs, spanwise uniformity of the transfer coefficients was examined by consecutive positioning of the active cylinder at all possible spanwise locations in a given row.

Axial pressure distributions were measured with the aid of 25 static taps deployed along the spanwise centerline of the upper wall of the duct. The tap locations will be evident from the pressure distribution results that will be presented later. The pressure signals from the taps were conveyed to a pressure selector switch via plastic tubing, and the output of the switch was read by a Baratron capacitance-type meter with a smallest scale reading of 0.001 mm Hg. For the measurement of the rate of air flow through the duct, either of two rotameters were employed, depending on the extent of the flow. To provide a well-defined inlet condition for the flow entering the duct, the entrance plane was framed with a baffle plate whose upstream face is flush with the exposed edges of the duct wall.

The extent of the mass transfer from the naphthalene-coated cylinders was measured with the aid of a Sartorius balance having a smallest scale reading of 0.01 mg.

Naphthalene-coated cylinders

The cylinders to be coated with naphthalene were cut from the same stainless steel rod stock and to the same length as those which were not coated. The coating was applied only to the portion of the cylinder that is exposed to the air stream (i.e. to both the exposed cylindrical surface and the exposed end face). The portion that is seated in the floor of the duct was left uncoated. As a preparatory step, the surfaces to be coated were undercut by about 0.025 cm (0.010 in) relative to the desired finished dimensions. On the undercut cylindrical wall, a fine screw thread (80 threads per in) was machined in order to provide recesses and grooves which aided the attachment of the naphthalene coating.

The coating procedure consisted of two processes: (a) application of the naphthalene and (b) machining to achieve the desired dimensions and surface finish. As a prelude to the coating process, the cylinder was thoroughly cleaned by immersion in acetone. Then, solid naphthalene was melted in a beaker and brought to a temperature just under the boiling point. The cylinder, held by tweezers which gripped the non-undercut portion, was dipped slowly into the molten naphthalene. At each dip, the cylinder was immersed for only a matter of seconds and then removed to allow the naphthalene to solidify. The dipping was repeated several times until a sufficiently thick coating was built up.

The machining was performed on a small bench lathe. A special collet was utilized to grip the uncoated portion of the cylinder; the collet was fitted with a stop which facilitated the attainment of the desired length dimension of the coated portion. A tool-bit turret containing two bits was utilized in the machining of the naphthalene. One of these bits was employed both for the rough and finish cuts on the end face and on the cylindrical surface. The function of the second bit (a knife-point bit) was to provide a sharply defined termination of the naphthalene coating at the boundary between the undercut and non-undercut portions of the cylindrical surface. Once this sharp demarcation had been made, any naphthalene that had inadvertently attached to the non-undercut portion of the surface was carefully removed.

The outcome of the machining was a naphthalene coating of excellent surface finish and closely held dimensions, with a square corner at the end of the cylinder. Typically, a number of coated cylinders were prepared in one batch to permit a succession of data runs to be performed in one day. When the machining was completed, the coated cylinders were wrapped in plastic to minimize extraneous sublimation. The cylinders were then placed in the laboratory to attain thermal equilibrium.

All aspects of the machining were performed with a high standard of cleanliness to avoid contamination of the surface of the coating.

Experimental procedure

As was noted earlier, only one of the cylinders in the array participated in the mass transfer process during a given data run. For each Reynolds number, a succession of runs was made in which the active cylinder was positioned in the first row during the first run, in the second row during the second run, etc. For each array (i.e. each cylinder height), experiments were performed for five Reynolds numbers. The pressure distribution measurements for each array were made in sets of runs separate from those for the mass-transfer measurements.

The naphthalene sublimed during a run was determined from measurements of the mass of coated cylinder made immediately before and after the run. The duration of a run was chosen so that the change in the mean diameter of the cylinder due to sublimation was about 0.0025 cm (0.001 in). For the three cylinder heights of the experiments, the corresponding change in mass is about 5, 10, and 15 mg, respectively. The run times corresponding to these changes in mass de-

pended on the Reynolds number and ranged from 15 to 65 min.

In the experiments, air was drawn into the apparatus from the temperature-controlled (~20°C), windowless laboratory room and was exhausted at the roof of the building. The outside exhaust ensured that the concentration of naphthalene vapor in the entering air was zero. The positioning of the blower downstream of the apparatus and outside of the laboratory avoided thermal disturbances.

Auxiliary experiments were performed to determine the possible extraneous loss of mass which might have occurred during the set-up of the apparatus (i.e. installation and removal of the coated cylinder) and during the weighing. Typically, the extraneous loss was on the order of 2%, and an appropriate correction was made.

DATA REDUCTION

Mass transfer

The measured change in mass of the coated cylinder, when corrected for extraneous sublimation and divided by the duration of the data run, yielded the mass-transfer rate $\dot{M}$. The mass transfer is driven by the difference between the concentrations of the naphthalene vapor at the surface of the cylinder and in the air approaching the cylinder. In the present experiments, the latter is zero. Then, upon denoting the former by ρ_{nw} and the mass-transfer area of the cylinder by A (the area includes both the cylindrical surface and the end face), a mass-transfer coefficient K can be defined as

$$K = \frac{\dot{M}/A}{\rho_{nw}}. \tag{1}$$

For the evaluation of the concentration ρ_{nw}, the Sogin vapor pressure–temperature relation [2] was employed in conjunction with the perfect gas law. The area appearing in equation [1] was evaluated as the mean between the areas at the beginning and the end of the data run.

The Sherwood number, which is the mass-transfer counterpart of the Nusselt number, was used for the dimensionless representation of the mass-transfer coefficients

$$Sh = KD/\mathscr{D} \tag{2}$$

in which D is the cylinder diameter and $\mathscr{D}$ is the naphthalene–air diffusion coefficient. The latter was evaluated from the Schmidt number $Sc = \nu/\mathscr{D}$, where $Sc = 2.5$ for naphthalene sublimation [2]. In view of the minute concentrations of the naphthalene vapor, ν was taken to be the kinematic viscosity of air.

With regard to the Reynolds number, considerable thought was given to the selection of an appropriate characteristic dimension and characteristic velocity. For the former, the cylinder diameter was chosen because it characterizes the size of the element from which the mass transfer is taking place. The selection of a characteristic velocity is a more complex issue because, as mentioned in the Introduction, the mean velocity in the open clearance space above the cylinders will differ from that in the inter-cylinder spaces. From the applications standpoint, it is highly unlikely that the velocity distribution would be known. Rather, only global information such as flow rates and dimensions would be available, and it appears reasonable to define a characteristic velocity using that information.

For consistency with heat exchanger practice, a superficial maximum velocity V_{max} will be defined as

$$V_{max} = \dot{w}/\rho A_{min} \tag{3}$$

where $\dot{w}$ is the mass flow rate through the entire cross section, and A_{min} is the minimum cross sectional area. A_{min} includes both the clearance space above the cylinders and the inter-cylinder spaces. With V_{max} as characteristic velocity, the Reynolds number is

$$Re = V_{max}D/\nu. \tag{4}$$

As an identification of the hydrodynamic state of the flow approaching the array, the duct Reynolds number Re_{duct} was also evaluated. If $\bar{V}$ is the mean velocity in the duct and D_h is the duct hydraulic diameter, then Re_{duct} may be written as

$$Re_{duct} = \bar{V}D_h/\nu. \tag{5}$$

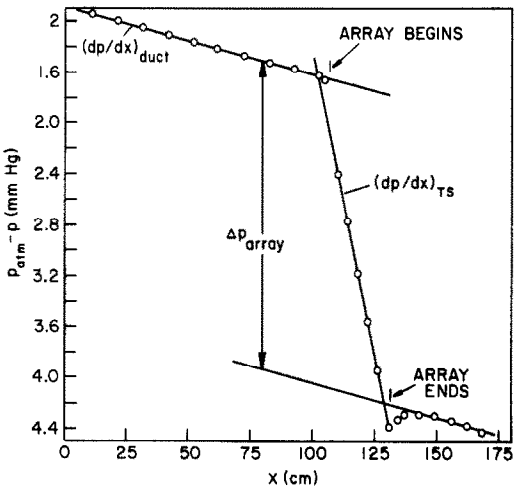

FIG. 2. Representative axial pressure distribution showing nomenclature for data reduction.

Pressure drop

For each operating condition characterized by a given Reynolds number and a given array, a plot of the axial pressure distribution was prepared, and Fig. 2 is typical of these plots (Fig. 2 corresponds to $h/D = 2$ and $Re = 5580$). The ordinate is the difference between the local pressure at x and the atmospheric pressure in the laboratory room, where x is the streamwise coordinate measured from the inlet cross section. The beginning and end points of the array are indicated in the figure.

The straight line passing through the data in the region upstream of the array corresponds to the fully developed pressure gradient for the unobstructed duct

flow. A parallel straight line was passed through the data in the region downstream of the array. In the absence of the array, the two lines would be co-linear. The vertical displacement, designated as Δp_{array}, is the net pressure drop due to the presence of the array—it is the pressure drop that is over and above that which would exist in the unobstructed duct. As defined here, Δp_{array} encompasses all pressure-related processes associated with the array, including entrance and exit effects as well as those internal to the array. The role of the entrance and exit effects will be discussed later.

To obtain a dimensionless representation of the pressure loss due to the array, a pressure coefficient K_p was defined as

$$K_p = \frac{\Delta p_{\text{array}}}{(\frac{1}{2}\rho V_{\max}^2) N}. \tag{6}$$

In this equation, $V_{\max}$ is the superficial maximum velocity defined by equation (3), ρ is the air density just upstream of the array, and N is the number of rows in the array.

The pressure data in the test section lie along a straight line whose slope is denoted by $(dp/dx)_{FS}$. The relation of this pressure gradient to Δp_{array} will be discussed later.

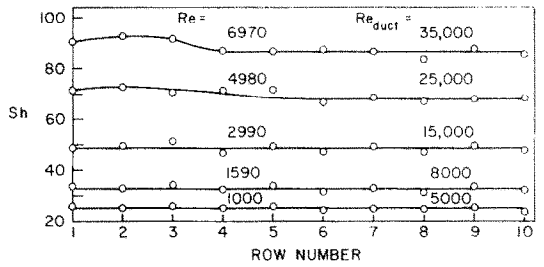

FIG. 3. Row-by-row Sherwood numbers, $h/D = 1$ and $h/H = 0.29$.

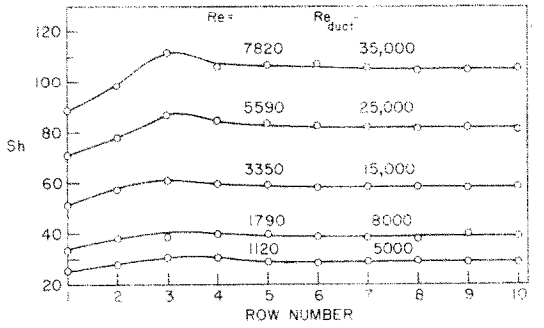

FIG. 4. Row-by-row Sherwood numbers, $h/D = 2$ and $h/H = 0.58$.

forward row and increases in the downstream direction. There are five sets of data in each figure, each corresponding to a specific Reynolds number, and numerical values are indicated for both the array Reynolds number Re and the duct Reynolds number Re_{duct}. Curves have been faired through the data points to provide continuity.

From an overall examination of Figs 3–5, several general characteristics of the results are in evidence. It may be observed that the transfer coefficient varies from row to row in the initial portion of the array and then takes on a constant value that is independent of position. Thus, in common both with flows in ducts and across tube banks, the cylinder array with tip clearance also displays entrance and fully developed regimes. The nature of the Sherwood number variation in the entrance region is not necessarily the same for all of the cases investigated, and the reasons for the differences will now be discussed.

From a broad perspective, two conflicting factors may be identified which influence the variation of the transfer coefficient in the entrance region. One of these factors is the row-by-row development of a pattern of

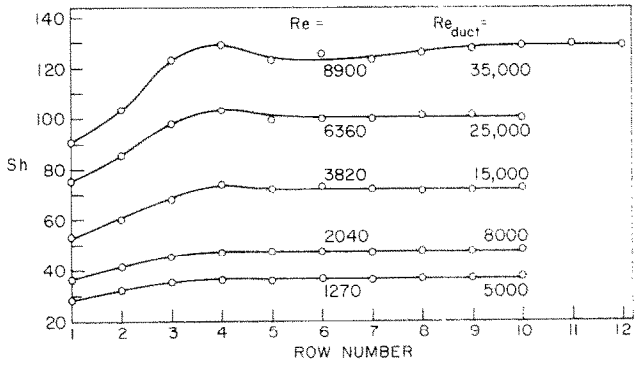

FIG. 5. Row-by-row Sherwood numbers, $h/D = 3$ and $h/H = 0.875$.

RESULTS AND DISCUSSION

Mass/heat transfer

The row-by-row mass-transfer results are presented in Figs 3, 4, and 5 for the respective arrays characterized by $h/D = 1, 2$, and 3. In each figure, the Sherwood number for each row is plotted as a function of the row number, where the numbering starts at the most flow acceleration and of wake shedding and impingement, both of which augment the transfer coefficients. The first row of cylinders in a staggered array is not impinged by wake flows nor are the fluid accelerations caused by the blockage of the cross section felt with their fullest effects. Although the second row is not washed by wakes, it is impinged by accelerated fluid

which has been channeled by the presence of the first row. The third row is impinged by wakes shed by the first row and by accelerated fluid channeled by the second row, and so forth. Thus, by thinking along these lines, a monotonic row-to-row increase of the transfer coefficient appears reasonable, ultimately culminating in a fully developed regime. Such a trend is applicable to tube bundles which span the entire flow cross section.

The second factor is the migration of flow from the relatively constrained inter-cylinder spaces to the open clearance space above the cylinders. This migration occurs in the initial part of the array and then ceases as the flow becomes hydrodynamically developed. The expected effect of the migration is a streamwise decrease in the transfer coefficient.

The conflicting effects of the two factors discussed in the preceding paragraphs, one tending to increase the transfer coefficient and the other tending to decrease it, give rise to the possibility of a local maximum. Such local maxima are in evidence in many for the distribution curves in Figs 3–5, especially at the higher Reynolds numbers for the intermediate and tallest cylinders. The transfer coefficients for the shortest cylinders are less affected by entrance region phenomena than are the others. In particular, there are no tangible entrance effects in evidence for the three lowest Reynolds numbers and there are only modest effects for the higher Reynolds numbers. In general, for all of the arrays, the entrance effects appear to be accentuated at higher Reynolds numbers.

The length of the entrance region depends both on the cylinder height and on the Reynolds number. If it is desired to have an overall indication of the entrance length which will serve for all cases, then, for practical purposes, the coefficients for the fourth and all subsequent rows can be regarded as being fully developed.

The one case which displays a somewhat unusual behavior is that for the tallest cylinders and the highest Reynolds number (Fig. 5, uppermost curve). For that case, it appears that there is a shallow local minimum prior to the attainment of the fully developed regime. Since the minimum is only about 4% below the fully developed value, it cannot be said with certainty whether the minimum reflects a flow field phenomenon or is merely data scatter.

There are two other general characteristics that may be identified in Figs 3–5. One of these is the expected increase of the transfer coefficients with increasing Reynolds number. The other (not necessarily expected) trend is that the transfer coefficients increase with increasing cylinder height for a fixed Reynolds number. This trend is the result of the changing relationship between the velocity in the inter-cylinder spaces and the cross sectional mean velocity which occurs as the cylinder height increases. For short cylinders, the inter-cylinder velocities are much less than the mean, whereas for taller cylinders the inter-cylinder velocities tend to approach the mean. Thus, the taller cylinders are washed by relatively higher velocities, which give rise to higher transfer coefficients.

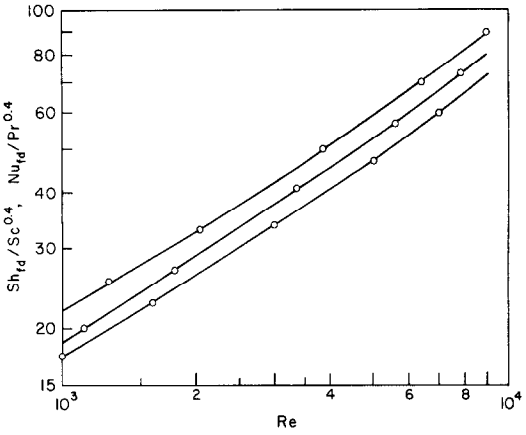

FIG. 6. Fully developed mass-/heat-transfer results.

The fully developed Sherwood numbers have been read from Figs 3–5 and are brought together in Fig. 6. With a view to generalizing the results, the quantity $Sh/Sc^{0.4}$ is plotted on the ordinate instead of Sh itself. The choice of $Sc^{0.4}$ as the scale factor rather than $Sc^{1/3}$ was based on two considerations. First, according to the most recent duct flow correlations, the dependence of Nu on Pr (or of Sh on Sc) is at least to the 0.4 power in the range of intermediate Pr ($\sim$0.7 to 2.5). Second, consistently better correlation between naphthalene sublimation results ($Sc = 2.5$) obtained in our laboratory for a variety of flows and corresponding heat-transfer results for air ($Pr = 0.7$) has been obtained with $Sc^{0.4}$ than with $Sc^{1/3}$.

According to the analogy between heat and mass transfer, a Nusselt–Reynolds–Prandtl correlation should be identical to a Sherwood–Reynolds–Schmidt correlation. Therefore, the ordinate of Fig. 6 has a dual label, $Sh_{fd}/Sc^{0.4}$ and $Nu_{fd}/Pr^{0.4}$, where fd denotes fully developed.

From an examination of Fig. 6, it is seen that for each array, the heat- or mass-transfer coefficients vary smoothly with the Reynolds number, increasing as Re increases. The curves that have been faired through the data are not straight lines, as is also the case for both single cylinders in crossflow and rod bundles. It is also seen that the transfer coefficients are larger for the taller cylinders, thereby affirming an observation made in connection with Figs 3–5.

It is appropriate to consider comparisons between the present results and any relevant literature information. As discussed in the Introduction, comparisons with the single set of heat transfer results for staggered pin fins given in the Kays–London compendium [1] do not appear to be apt. This is not only because of the trip wire effect cited there, but also because the transfer coefficients of [1] encompass the duct walls as well as the pin fins. Nevertheless, when comparisons were made (the results of [1] were scaled by $Pr^{0.4}$), the present results for the tallest cylinders fell about 25% below the transfer coefficients of [1]. In view of the differences between the cases being compared, this level of agreement is surprisingly good.

Comparison of the present results with available

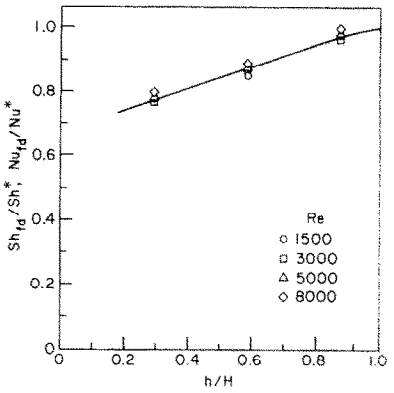

FIG. 7. Comparison of present fully developed mass-/heat-transfer results with those for a tube bank.

heat-transfer results for tube banks in crossflow appears to be appropriate since the two cases should approach each other when the cylinders are sufficiently tall. Tube bank results corresponding to the appropriate longitudinal and transverse spacing ratios were taken from the compendium of Fraas and Ozisik [3], Fig. H5.12(a) and scaled by $Pr^{0.4}$; these results are designated as Sh^* (or Nu^*). The present fully developed Sherwood numbers were read from Fig. 6 at Reynolds numbers convenient for the comparison. The thus-evaluated ratios of Sh_{fd}/Sh^* (and, by analogy, of Nu_{fd}/Nu^*) are plotted in Fig. 7 as a function of h/H—the ratio of the cylinder height to the duct height.

It is remarkable to observe that even for the shortest cylinders, the Sherwood (Nusselt) number is not markedly different from Sh^* (Nu^*), the deviation being in the 20% range. For the tallest cylinders, the Sherwood numbers are within a few per cent of Sh^*. If this finding is viewed optimistically, it would appear that tube-bank Nusselt numbers can serve as a first approximation in the design of cylinder arrays such as pin fins. However, this optimism has to be tempered by the realization that Sh and Nu^* respectively represent local and overall results. Also, the accuracy of the overall measurements may not be commensurate with that of the local measurements.

As a final remark with regard to the mass-transfer results, it may be noted that spanwise distributions, measured in auxiliary runs, were uniform to within the typical scatter of the data.

Pressure drop

The dimensionless per-row pressure drop due to the presence of the cylinder array is expressed by the pressure coefficient K_p defined by equation (6). The measured values of K_p are listed in Table 1, where the array designation h/D parameterizes consecutive pairs of columns and the Reynolds numbers are listed vertically. The average value of K_p for each array is indicated at the bottom of the table.

From the table, it is seen that aside from data scatter, K_p appears to be independent of the Reynolds number for each array, so that the respective average values constitute a meaningful representation of the results. On the other hand, K_p is strongly affected by the height

Table 1. Pressure coefficient per row, K_p

$h/D = 1$		$h/D = 2$		$h/D = 3$	
Re	K_p	Re	K_p	Re	K_p
1000	0.0382	1120	0.139	1270	0.297
1590	0.0382	1790	0.126	2040	0.286
2990	0.0396	3350	0.128	3820	0.287
4980	0.0382	5590	0.122	6360	0.281
6970	0.0405	7820	0.123	8900	0.269
Average	0.0389		0.128		0.284

of the cylinders and increases by about a factor of seven over the range from $h/D = 1$ to $h/D = 3$. The K_p value for the tallest cylinders is within 10% of that for a corresponding tube bank {[3], Fig. H5.12(a)}.

As was noted earlier, Δp_{array} (and its dimensionless counterpart K_p) represents a pressure drop which is over and above that which would exist in the unobstructed duct. Therefore, the total pressure drop which is sustained when the array is in place is the sum of Δp_{array} and the pressure drop of the unobstructed duct. Thus, for a duct length L (L includes the streamwise length of the array), the total pressure drop is

$$\Delta p_{\text{array}} + L|\mathrm{d}p/\mathrm{d}x|_{\text{duct}}. \tag{7}$$

The duct pressure gradients measured in the present experiments are in very good agreement with those given by standard friction factors (e.g. [4]).

It is of interest to compare the relative magnitudes of the two terms in equation (7) for a length L_{TS} equal to that of the test section (i.e. the streamwise length of the array). For this length, the ratio of the duct pressure drop (the second term) to Δp_{array} was found to be about 25, 6, and 2%, respectively for the arrays with $h/D = 1$, 2, and 3 ($h/H = 0.29, 0.58$, and 0.875). Thus, within the test section itself, the pressure drop due to the array is the major contributor to the total pressure drop.

Another approach to evaluating the total pressure drop in the test section is via

$$L_{TS}|\mathrm{d}p/\mathrm{d}x|_{TS} \tag{8}$$

where $|\mathrm{d}p/\mathrm{d}x|_{TS}$ is the pressure gradient in the test section as determined from graphs such as Fig. 2. The pressure drop given by equation (8) should differ from that evaluated from equation (7) with $L = L_{TS}$ because Δp_{array} includes entrance and exit effects whereas $L_{TS}|\mathrm{d}p/\mathrm{d}x|_{TS}$ is strictly internal to the test section. Therefore, the difference between the pressure drops respectively given by equations (7) and (8) provides an indication of the importance of the entrance and exit effects. The average of the absolute magnitudes of the differences, taken over all cases, was only 3%, and the extreme difference was about 6½%. These results indicate that Δp_{array} was not significally affected by entrance and exit effects and, correspondingly, neither is K_p.

CONCLUDING REMARKS

The present research on wall-attached cylinder arrays with tip clearance extends the naphthalene

sublimation technique to a situation markedly different from those to which it has been applied in the past. To have dealt with this situation directly as a heat-transfer experiment would have been much more difficult, and it is doubtful if results could have been obtained of comparable accuracy to those of the naphthalene experiments.

The row-by-row transfer coefficients were found to vary only in the initial rows and to attain a constant fully developed value thereafter. For practical purposes, the transfer coefficients for the fourth and all subsequent rows can be regarded as fully developed. The array with the shortest cylinders (i.e. largest tip clearance) was least influenced by entrance effects.

The dimensionless fully developed mass-transfer coefficients, represented in terms of the Sherwood number, were recast as Nusselt numbers via the analogy between heat and mass transfer. These coefficients were found to be relatively insensitive to the height of the cylinders, increasing by only about 20% as h/D varied from 1 to 3 and h/H varied from 0.29 to 0.875. Furthermore, the transfer coefficients for the tallest cylinders showed good agreement with those for a tube bank having the same longitudinal and transverse spacing ratios.

Experiments were also performed to determine the incremental pressure drop due to the presence of the array, over and above that for the unobstructed duct. The pressure drop was normalized by the velocity head and reported on a per-row basis. In contrast to the mass- or heat-transfer coefficients, the array pressure drop increased by a large multiple with increasing cylinder height.

Acknowledgements—This research was performed under the auspices of NSF grant ENG77-06762. The assistance of Mr. Gregory D. Halvorson is gratefully acknowledged.

REFERENCES

1. W. M. Kays and A. L. London, *Compact Heat Exchangers*, 2nd edn. McGraw-Hill, New York (1964).
2. H. H. Sogin, Sublimation from disks to airstreams flowing normal to their surfaces, *Trans. Am. Soc. Mech. Engrs* **80**, 61–69 (1958).
3. A. P. Fraas and M. N. Ozisik, *Heat Exchanger Design*. John Wiley, New York (1965).
4. O. C. Jones Jr., An improvement in the calculation of turbulent friction in rectangular ducts, *J. Fluids Engng* **98**, 173–180 (1976).

TRANSFERT THERMIQUE ET PERTE DE PRESSION POUR UN ARRANGEMENT ETAGE DE CYLINDRES SOLIDAIRES D'UNE PAROI AVEC ESPACEMENT DES EXTREMITES

Résumé—Des expériences ont été conduites pour déterminer les caractéristiques de transfert thermique détaillé rangée par rangée d'un ensemble de cylindres circulaires placés dans un courant d'air transversal à l'intérieur d'un canal rectangulaire. Les cylindres sont fixés perpendiculairement à l'une des parois du canal, avec espacement des extrémités libres des cylindres et de l'autre paroi en vis-à-vis. Les coefficients de transfert thermique sont obtenus en appliquant l'analogie entre les transferts de masse et de chaleur à partir de la mesure de la sublimation du naphtalène. Des mesures de pression ont été faites pour déterminer la perte de pression due à la présence des cylindres. Les coefficients de transfert rangée par rangée varient seulement dans les premières rangées et atteignent une valeur constante à partir de la quatrième. Les coefficients du régime établi sont insensibles à la hauteur du cylindre (c'est à dire à la valeur de l'espacement des extrémités), croissant modérément lorsque la hauteur augmente (l'espacement diminue). D'autre part, la perte de pression croît de façon marquée quand la hauteur des cylindres augmente.

WÄRMEÜBERGANG UND DRUCKVERLUST FÜR AN EINER WAND BEFESTIGTE ZYLINDER IN VERSETZTER ANORDNUNG MIT EINER FREIN STIRNFLÄCHE

Zusammenfassung—Es wurden Experimente durchgeführt zur Untersuchung des Wärmeübergangs an den einzelnen Reihen einer versetzten Anordnung von Kreiszylindern, die in einem flachen, rechtwinkligen Kanal quer von Luft angeströmt werden. Die Zylinder sind senkrecht an einer Hauptwand des Kanals befestigt mit einem freien Raum zwischen den freien Enden der Zylinder und der anderen Hauptwand. Man erhielt die Wärmeübergangskoeffizienten durch Anwendung der Analogie zwischen Wärme- und Stoffübergang als Stoffübergangskoeffizienten, die mittels der Naphthalin-Sublimations-Technik gemessen wurden. Ebenfalls wurden Druckmessungen durchgeführt, um den zusätzlichen Druckverlust durch die Zylinderanordnung zu bestimmen. Es wurde festgestellt, daß die Übergangskoeffizienten der einzelnen Reihen nur in den ersten Reihen variieren und für die vierte und alle folgenden Reihen einen konstanten, voll ausgebildeten Wert erreichen. Die Koeffizienten für den voll ausgebildeten Übergang sind ziemlich unabhängig von der Zylinderhöhe (d. h. vom freien Abstand der Zylinderstirnflächen zur Kanalwand), wobei sie mäßig mit größer werdener Höhe (und kleiner werdendem freien Zwischenraum) zunehmen. Andererseits nimmt der Druckverlust mit größer werdender Zylinderhöhe deutlich zu.

ПЕРЕНОС ТЕПЛА И ПЕРЕПАД ДАВЛЕНИЯ В ПУЧКЕ ЦИЛИНДРОВ, ОДНИМ КОНЦОМ ПРИКРЕПЛЕННЫХ К СТЕНКЕ КАНАЛА И РАСПОЛОЖЕННЫХ В ШАХМАТНОМ ПОРЯДКЕ

Аннотация — Проведены эксперименты по определению характеристик теплообмена между рядами пучка круглых цилиндров, расположенных в шахматном порядке и обтекаемых поперечным потоком воздуха в плоском прямоугольном канале. Одним концом цилиндры присоеденены перпендикулярно к одной из вертикальных стенок канала. Между свободными концами цилиндров и другой вертикальной стенкой имеется зазор. Коэффициенты теплообмена определялись по аналогии между тепло- и массообменом через коэффициенты массообмена, определяемые методом сублимации нафталина. Проведены также измерения перепада давления в пучке. Коэффициенты переноса в пучке изменяются в начальных рядах, достигая постоянного значения в четвертом ряду. Значения коэффициентов переноса для четвертого и последующего рядов почти не зависят от высоты цилиндров (т. е. от величины зазора между свободными концами цилиндров и стенкой) и незначительно возрастают с ростом высоты цилиндров (с уменьшением зазора). С другой стороны, перепад давления в пучке заметно увеличивается с увеличением высоты цилиндров.